

π -Conjugated Trinuclear Group-9 Metalladithiolenes with a Triphenylene Backbone

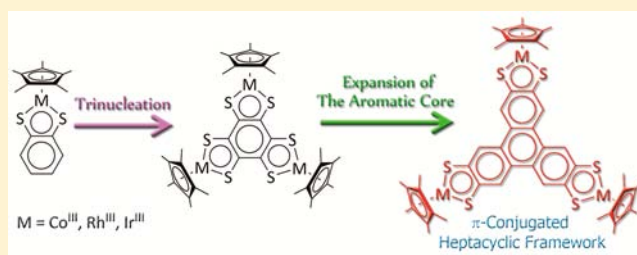
Ryota Sakamoto,^{*,†} Tetsuya Kambe,[†] Satoru Tsukada,[†] Kenji Takada,[†] Ken Hoshiko,[†] Yasutaka Kitagawa,[‡] Mitsutaka Okumura,[‡] and Hiroshi Nishihara^{*,†}

[†]Department of Chemistry, Graduate School of Science, The University of Tokyo, 7-3-1, Hongo, Bunkyo-ku, Tokyo 113-0033, Japan

[‡]Department of Chemistry, Graduate School of Science, Osaka University, 1-1 Machikaneyama, Toyonaka, Osaka 560-0043, Japan

S Supporting Information

ABSTRACT: Previously, we synthesized π -conjugated trinuclear metalladithiolene complexes based on benzenehexathiol (J. Chem. Soc., Dalton Trans. **1998**, 2651; Dalton Trans. **2009**, 1939; Inorg. Chem. **2011**, *50*, 6856). Here we report trinuclear complexes with a triphenylene backbone. A reaction with triphenylenehexathiol and group 9 metal precursors in the presence of triethylamine gives rise to trinuclear complexes 9–11. The planar structure of 11 is determined using single crystal X-ray diffraction analysis. The ligand-to-metal charge transfer bands of 9–11 move to longer wavelengths compared with those of mononuclear 12–14. Electrochemical measurements disclose that the one-electron and two-electron reduced mixed-valent states are stabilized thermodynamically. UV–vis–NIR spectroscopy for the reduced species of 9 identifies intervalence charge transfer bands for 9⁻ and 9²⁻, substantiating the existence of electronic communication among the three metal nuclei. These observations prove that the triphenylene backbone transmits π -conjugation among the three metalladithiolene units.



INTRODUCTION

Multinuclear transition metal complexes have attracted attention of chemists because they exhibit interesting properties such as mixed-valent (MV) states, spin frustration, catalytic activity, and unique chemical reactivities.^{1–3} Some of the features are attributed to electronic and magnetic interactions among the metal centers, which occur through bridging entities. π -Conjugated bridges in particular allow multinuclear metal complexes to exhibit long-range and strong interactions among their metal nuclei.^{3c,e} Recently, we reported the multinucleation of metalladithiolene complexes and cluster complexes.^{4,5} A considerable portion of this work involved π -conjugated trinuclear metalladithiolene complexes composed of benzenehexathiol (BHT) (Figure 1).⁴ Thanks to the quasi-aromaticity of the metalladithiolene five-membered ring, the phenylene bridge and three metalladithiolene rings formed a highly planar tetracyclic framework, featuring high levels of π -conjugation (1–8, Figure 1a).⁴ The π -conjugated framework allowed intense electronic communication among the metal centers in the MV states.

Triphenylene is distinctive among polyaromatic hydrocarbons (PAHs), as it shows 3-fold symmetry, a vast π -conjugation plane, and strong aromatic resonance stabilization.⁶ These features are beneficial in, for example, highly conductive discotic liquid crystals made of *S*-alkylated 2,3,6,7,10,11-triphenylenehexathiol (THT).⁷

This article addresses the synthesis of trinuclear metalladithiolene complexes 9–11 with group 9 metals (Figure 1a).

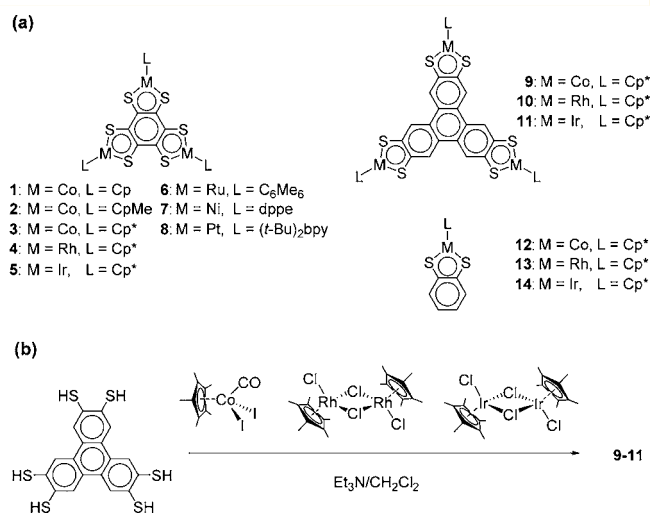


Figure 1. (a) π -Conjugated metalladithiolenes: Trinuclear complexes with phenylene (1–8) and triphenylene (9–11) bridging units, and mononuclear complexes (12–14). (b) Synthetic scheme for 9–11.

We expected that the resultant π -conjugated heptacyclic framework would allow electronic interactions to be communicated among the metal nuclei over longer distances

Received: January 16, 2013

Published: June 12, 2013

than in BHT-based trinuclear metalladithiolene complexes. The synthesis, crystal structure, UV–vis–NIR absorption spectra, density functional theory (DFT) calculation, electrochemistry, and electronic communication in the reduced MV states were investigated. Reports of metal complexes based on a THT platform are rare,⁸ and none has yet employed the metalladithiolene motif. We also note that there are reports on multinuclear ruthenium complexes having hexaazatriphenylene⁹ and hexahydroxytriphenylene¹⁰ ligands. They undergo ligand-based oxidations and reductions. This is in sharp contrast to our present research, focusing on the reduction and MV state of the metal center.

RESULTS AND DISCUSSION

Synthesis and Identification. The synthetic procedure for 9–11 is shown in Figure 1b. The addition of THT to dichloromethane solutions of $[\text{Cp}^*\text{Co}(\text{CO})\text{I}_2]$, $[(\text{Cp}^*\text{RhCl}_2)_2]$, and $[(\text{Cp}^*\text{IrCl}_2)_2]$ (Cp^* = pentamethylcyclopentadienyl group) in the presence of triethylamine gave rise to target trinuclear complexes 9–11 (see experimental section for details). In addition to general characterization measurements, 9–11 were subjected to X-ray photoelectron spectroscopy (XPS), which revealed the constitutive elements (Figure 2).

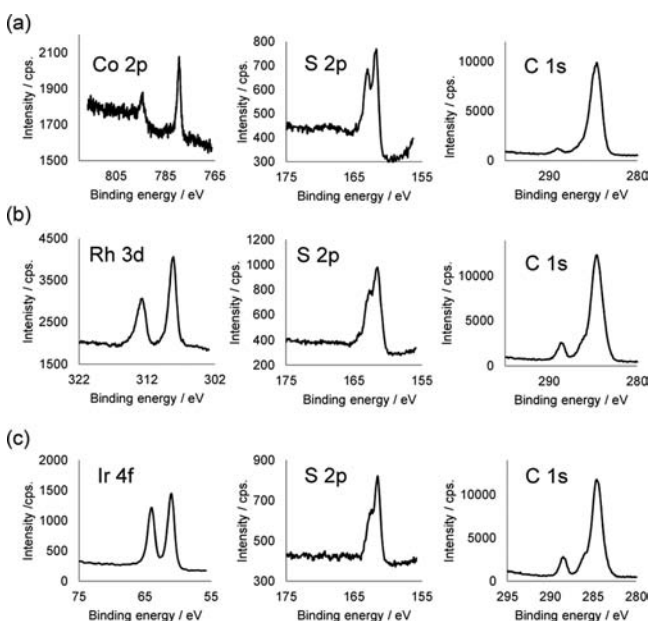


Figure 2. X-ray photoelectron spectra of (a) 9, (b) 10, and (c) 11.

Single Crystal X-ray Structure Analysis. Single crystals of 11 suitable for X-ray diffraction analysis were obtained via recrystallization from dichloromethane/hexane at room temperature; the ORTEP¹¹ drawing and crystal packing are shown in Figure 3, and the crystallographic parameters are detailed in Supporting Information, Table S1. We note that this is the first crystal structure reported for a trinuclear metalladichalcogenolene complex based on a triphenylene backbone. All iridium ions form five-membered iridadithiolene rings, which are fused with each other via the central triphenylene core. The bond lengths relating to the iridadithiolene ring (Ir–S, 2.248 Å; S–C, 1.77 Å; C–C, 1.35 Å) are almost identical to those of BHT-bridged 5 (Ir–S, 2.25 Å; S–C, 1.75 Å; C–C, 1.37 Å).^{4b} Apart from the Cp^* rings, 11 features a planar heptacycle with a slight bend. The bend stems from intermolecular packing between

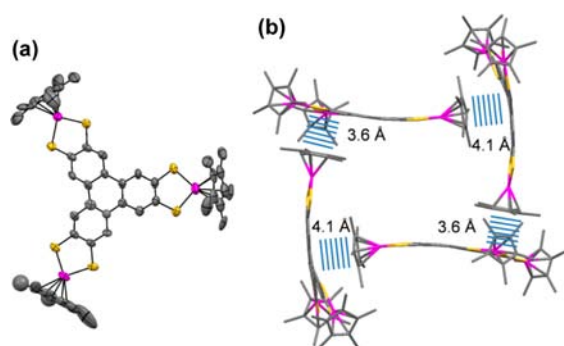


Figure 3. (a) ORTEP drawing of 11 with a thermal ellipsoid set at the 50% probability level. (b) Crystal packing structure of 11 (gray, C; yellow, S; and pink, Ir). Hydrogen atoms and crystal solvents are omitted for clarity.

the Cp^* ring and triphenylene core, which forms a tetrameric assembly (Figure 3b).

UV–vis–NIR Absorption Spectroscopy. Absorption spectra for 9–11 in dichloromethane are shown in Figure 4a:

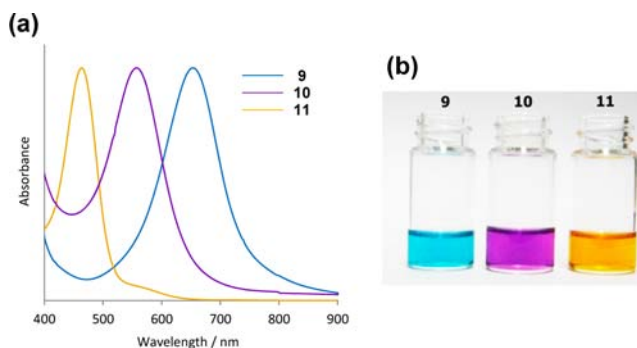


Figure 4. (a) UV–vis–NIR absorption spectra (normalized) and (b) photos of dichloromethane solutions of THT-bridged trinuclear complexes 9–11.

The wavelength (λ_{max}) and molar extinction coefficient (ϵ_{max}) at the absorption maxima are summarized in Table 1, along

Table 1. λ_{max} and ϵ_{max} for the ¹LMCT of 3–5 and 9–14

compound	$\lambda_{\text{max}}/\text{nm}$	$10^{-4} \epsilon/\text{M}^{-1} \text{cm}^{-1}$
9	653	3.67
10	557	2.38
11	464	5.60
3 ^a	704	3.21
4 ^a	590	3.62
5 ^a	499	3.61
12	574	0.93
13	500	0.76
14	418	1.06

^aFrom ref 4b.

with those of 3–5, and corresponding mononuclear complexes 12–14 (Figure 1a). 9–11 feature intense absorptions in the visible and NIR region, which are reflected in the vivid solution color (Figure 4b). According to knowledge on the mononuclear complexes, these absorptions are assigned to singlet ligand-to-metal charge transfer (¹LMCT) transitions.^{4b} The ¹LMCT band of 11 has a shoulder at around 570 nm, which is presumably derived from the ³LMCT transition induced by the

heavy atom effect of the iridium center. The $^1\text{LMCT}$ bands of THT-bridged trinuclear **9–11** are red-shifted compared with those of mononuclear **12–14**, but the redshift is less prominent than that associated with BHT-bridged trinuclear **3–5**.

DFT Calculation. To elucidate the result of UV–vis–NIR absorption spectroscopy, DFT calculations were conducted. First, results for cobalt complexes **3**, **9**, and **12** are discussed (Figure 5 and Supporting Information, Figure S1 and Table

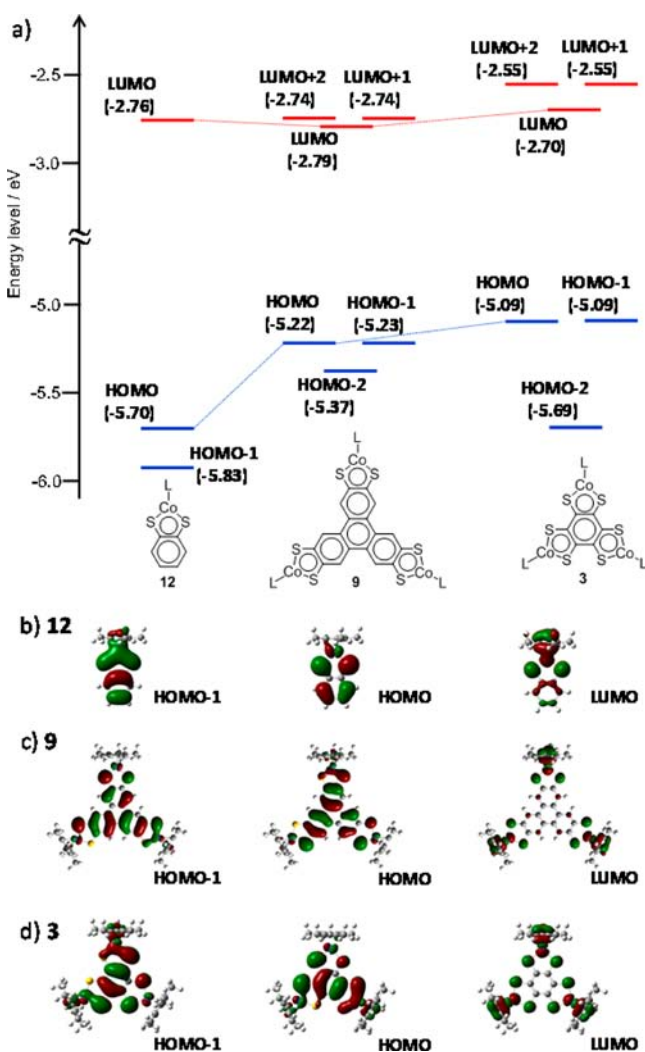


Figure 5. (a) Frontier orbital diagrams for **12**, **9**, and **3**, estimated using DFT calculation. (b) HOMO-1, HOMO, and LUMO for **12**. (c) HOMO-1, HOMO, and LUMO for **9**. (d) HOMO-1, HOMO, and LUMO for **3**.

S2). The highest occupied molecular orbital (HOMO) and HOMO-1 of **12** originate from the cobaltadithiolene(π) (Figure 5b). Similarly, the cobaltadithiolene(π) orbitals from the three dithiolene units are responsible for the HOMO, HOMO-1, and HOMO-2 in **3** and **9** (Figure 5c,d, and Supporting Information, Figure S1). The HOMO and HOMO-1 levels of **3** and **9** are subject to destabilization compared with the HOMO level of **12**, which is caused by π -conjugation transmitted by the triphenylene and phenylene cores (Figure 5a). The destabilization is more significant in **3** than in **9**, indicative of the distance decay of the π -conjugation. On the other hand, the lowest unoccupied molecular orbital (LUMO) of **12** receives a substantial contribution from the vacant Co(d)

(Figure 5b). The same is true for the LUMO, LUMO+1, and LUMO+2 of **3** and **9** (Figure 5c,d). Unlike the HOMOs, the stabilization of the LUMOs in **3** and **9** over the LUMO in **12** is not significant (Figure 5a).

3, **9**, and **12** were also subjected to time-dependent DFT (TDDFT) calculations. The visible and NIR absorption of **12** is governed by the HOMO-1 \rightarrow LUMO transition (Supporting Information, Tables S3 and S4). Similarly, those of **9** and **3** comprise the HOMO-1 \rightarrow LUMO and HOMO \rightarrow LUMO transitions (Supporting Information, Tables S5–S8). This is consistent with the previous assignment that the visible-NIR band is $^1\text{LMCT}$.^{4b} The estimated absorption wavelength is in the order of $12 < 9 < 3$ (Supporting Information, Tables S3–S8), which is consistent with the order observed experimentally in UV–vis–NIR spectroscopy (Table 1). The destabilization of the HOMO and HOMO-1, cobaltadithiolene(π), contributes to the redshift of the $^1\text{LMCT}$ in trinuclear **9** and **3** (Figure 5a).

We also conducted DFT and TD-DFT calculations for THT-bridged trinuclear Rh and Ir complexes **10** and **11**. The result is summarized briefly in combination with that of Co complex **9**. The metal center does not affect the nature of the frontier orbitals (Supporting Information, Figure S2 and Table S9). The main transition in the visible and NIR band is also invariant, $^1\text{LMCT}$ (Supporting Information, Tables S10–S13). The order of the absorption maximum is in the order of $11 < 10 < 9$: this is attributed to the destabilization of the LUMO, the vacant metal(d) orbital, in 5d Ir and 4d Rh over 3d Co, which is demonstrated clearly by means of electrochemistry (vide infra).

Electrochemistry. Figure 6 and Table 2 give details and results for the electrochemical measurements performed for **9–**

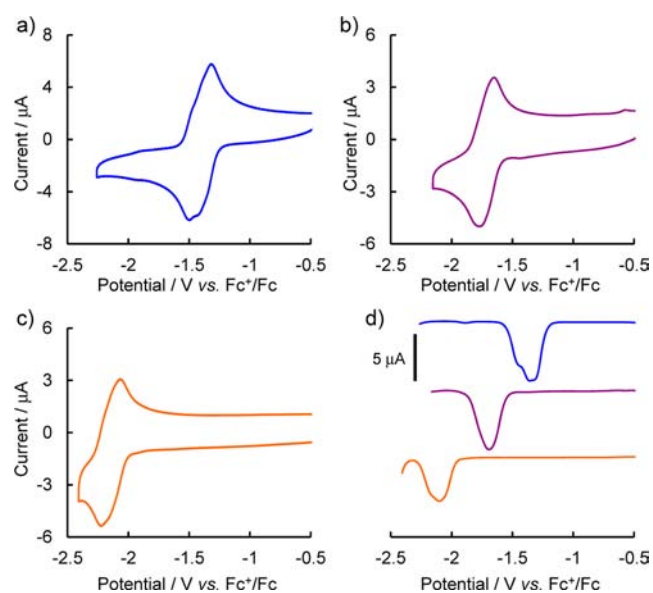


Figure 6. Cyclic voltammograms for (a) **9**, (b) **10**, and (c) **11**, measured at a scan rate of 100 mV s^{-1} in $0.1 \text{ M } n\text{-Bu}_4\text{NClO}_4\text{-PhCN}$ at 298 K , and (d) differential pulse voltammograms for **9–11** measured under the same conditions.

11 in $0.1 \text{ M } n\text{-Bu}_4\text{NClO}_4\text{-PhCN}$ at room temperature. As a reference, the results for **3–5** and **12–14** are reproduced in Table 2. **9–11** all show reversible reductions. Differential pulse voltammograms (Figure 6d) and their deconvolution (Supporting Information, Figure S3) disclose that the reduction wave is composed of three one-electron reductions. Judging from the DFT calculations described above and the previous result on

Table 2. Formal Potentials (E°) and Comproportionation Constants (K_c) for the Reduction of 3–5 and 9–14

compd.	potential/V vs Fc ⁺ /Fc			comproportionation constant	
	$E^{\circ}(\text{X}^{2-}/\text{X}^{3-})$	$E^{\circ}(\text{X}^-/\text{X}^{2-})$	$E^{\circ}(\text{X}/\text{X}^-)$	$\log K_c(\text{X}^{2-})$	$\log K_c(\text{X}^-)$
9	-1.46	-1.38	-1.31	1.4	1.2
10	-1.76	-1.70	-1.64	1.0	1.0
11	-2.18	-2.11	-2.05	1.2	1.0
3 ^a	-1.92	-1.58	-1.35	5.8	3.9
4 ^a	-2.18	-1.93	-1.74	4.2	3.2
5 ^a	-2.35	-2.21	-2.12	2.4	1.5
12			-1.42		
13			-1.74		
14			-2.11		

^aFrom ref 4b.

metalladithiolenes with group 9 metals,^{4b} the series of reductions is derived from the three metal centers. In addition, the stepwise reduction of the three equivalent metal centers indicates that the MV species (i.e., X^- and X^{2-}) are stabilized thermodynamically. The comproportionation constants $K_c(\text{X}^-)$ and $K_c(\text{X}^{2-})$,^{12a} are described by eqs 1 and 2

$$K_c(\text{X}^-) = \frac{[\text{X}^-]^2}{[\text{X}][\text{X}^{2-}]} = \exp[(E^{\circ}(\text{X}/\text{X}^-) - E^{\circ}(\text{X}^-/\text{X}^{2-}))F/RT] \quad (1)$$

$$K_c(\text{X}^{2-}) = \frac{[\text{X}^{2-}]^2}{[\text{X}^-][\text{X}^{3-}]} = \exp[(E^{\circ}(\text{X}^-/\text{X}^{2-}) - E^{\circ}(\text{X}^{2-}/\text{X}^{3-}))F/RT] \quad (2)$$

where $[\text{X}^n]$ is the concentration of chemical species X^n , and $E^{\circ}(\text{X}^{n+1}/\text{X}^n)$ is the formal potential of the $\text{X}^{n+1}/\text{X}^n$ redox couple. The $\log K_c$ values are collected in Table 2. These values suggest that the stabilization of the MV states in 9–11 is smaller than that in 3–5 because of the distance attenuation (intermetal distance: 11.71 Å for 9, and 7.41 Å for 3, from DFT calculations), but is still appreciable.

Electronic Communication. Electronic communication in MV states surely has a positive contribution to K_c , though, other factors such as a Coulombic contribution make K_c an unreliable measure for electronic communication.^{12b–f} We reported previously that 3–5 enjoyed electronic communication among the three metal nuclei in the reduced MV states.^{4a,b} Here we also investigate electronic communication in 9 by means of chemical reduction using a sodium mirror, followed by UV–vis–NIR spectroscopy. A three-step UV–vis–NIR spectral change corresponds to $9 \rightarrow 9^- \rightarrow 9^{2-} \rightarrow 9^{3-}$ (Supporting Information, Figure S4). Among these species, MV 9^- and 9^{2-} show a weak but broad absorption in the NIR region (900–1500 nm). The NIR absorption is assignable to an intervalence charge transfer (IVCT) band. Unfortunately, we cannot quantify the off-diagonal matrix coupling element H_{ab} using Hush's equation¹³ because the reduction of the ¹LMCT band overlaps on the IVCT band significantly. We note that a trinuclear cobalt complex based on benzenehexathiol **1** also showed disappearance of the ¹LMCT band upon reduction to I^- , I^{2-} , and I^{3-} .^{4a} Nevertheless, we can still conclude that **9** expresses electronic communication over the long distance, which is transmitted by the π -conjugated triphenylene core.

CONCLUSIONS

Cyclic trinuclear metalladithiolenes complexes of group 9 metals **9–11** are synthesized using THT as a π -bridging ligand. The single crystal X-ray structure of **11** features a planar π -conjugated heptacyclic framework. **9–11** possess intense absorptions in the visible and NIR region, which are assigned to ¹LMCT transitions. The ¹LMCT bands of **9–11** are red-shifted compared with those of the corresponding mononuclear complexes **12–14**. **9–11** undergo successive three one-electron reductions with respect to the metal nuclei. Chemically reduced 9^- and 9^{2-} show IVCT bands in the NIR region, which indicates that the metal nuclei possess electronic communication. These experimental facts prove that the triphenylene core transmits π -conjugation among the three metalladithiolenes units.

EXPERIMENTAL SECTION

General Procedures. All reactions were carried out under an argon or a nitrogen atmosphere. Column chromatography was performed using Silica Gel 60 N (Kanto Chemicals, spherical, neutral) or Aluminum oxide 90 (Merck, basic). ¹H (500 MHz) and ¹³C (126 MHz) NMR spectra were recorded on Bruker-DRX500 spectrometer using $\text{CHCl}_3/\text{CDCl}_3$ (δ_{H} 7.25, δ_{C} 77.00) or $\text{CDHCl}_2/\text{CD}_2\text{Cl}_2$ (δ_{H} 5.32, δ_{C} 53.84) as an internal standard. MALDI-TOF-MS and ESI-TOF-MS were recorded on Shimadzu/KRATOS AXIMA CFR spectrometer and Waters LCTPremierXE spectrometer, respectively. UV–vis–NIR spectra were recorded on JASCO V-570 spectrometer. XPS was obtained using PHI 5000 VersaProbe (ULVAC-PHI, INC.). Al K α (15 kV, 25 W) was used as an X-ray source, and the beam was focused on a 100- μm^2 area. The spectra were analyzed using MultiPak Software and standardized using a peak of C(1s) emerging at 284.6 eV. The sample was immobilized on the sample stage using a conductive adhesive tape. X-ray diffraction data were collected using Rigaku VariMax with Rigaku Saturn CCD system equipped with a rotating-anode X-ray generator that emits graphite-monochromated MoK α radiation (0.7107 Å). Empirical absorption corrections using equivalent reflections and Lorentzian polarization correction were performed using Crystal Clear 1.3.6. The structures were solved using SHELXS-97 and refined against I^2 using SHELXL-97.¹⁴

DFT Calculation. DFT and TDDFT calculations were performed on Gaussian 09.¹⁵ All optimized structures were obtained at B3LYP level of theory. As the basis sets, 6-31G* is used for complexes **3**, **9**, and 6-31+G* for **12**, respectively. For the complexes **10** and **11**, LanL2TZf and 6-31+G* basis sets are used for the metal ions and ligands, respectively. Molecular orbitals and excited states were obtained at the B3LYP/6-31+G* for complexes **3**, **9**, and **12**, and B3LYP/(LanL2TZf, 6-31+G*) for **10**, **11**. The solvent effect (dichloromethane) was considered using the PCM method.¹⁶ For the full geometry optimization of the complexes, all symmetry restrictions are turned off during the computation. The C_{3v} symmetry of the trinuclear complexes becomes C_1 because Cp* ligands are slightly rotated cooperatively against the symmetry. Owing to the lower molecular symmetry, the irreducible representations of the molecular orbitals are not available.

Electrochemistry. Cyclic voltammetry and differential pulse voltammetry were performed on BAS ALS750A analyzer. A glassy carbon disc electrode was used as a working electrode, a platinum wire as a counter electrode, and an Ag^+/Ag (0.01 M AgClO_4 in 0.1 M $n\text{-Bu}_4\text{NClO}_4/\text{acetonitrile}$) homemade electrode as a reference electrode. Ferrocene was used as an internal standard. The concentration of the samples was 0.5 mM, and the solution was degassed by Ar bubbling.

Chemical Reduction of 9. A 10 mm \times 10 mm quartz spectrometric cell was equipped with a pyrex glass tube appended by glass branches. After **9** and Na were placed in one branch and another branch, respectively, the glassware was connected to a high vacuum line. A sodium mirror was deposited by depressurization, and tetrahydrofuran (THF) was transferred to the branch holding **9** by

vacuum distillation. Finally, the glassware was sealed off. Stepwise reduction of **9** was carried out by contacting the sample solution with the sodium mirror iteratively. UV–vis–NIR spectroscopy was conducted by transferring the sample solution to the spectrometric cell.

Materials. Dichloromethane was purchased from Asahi Glass Co. Ltd. Hexane was purchased from Kanto Chemicals. All solvents were distilled from calcium hydride and dried over molecular sieves 4A. Lithium (ribbon) was purchased from Sigma-Aldrich Co. Triethylamine was purchased from Kanto Chemicals. Hexamethylthiotriphenylene,¹⁷ Cp*Co(CO)I₂,^{18,19} (Cp*RhCl₂)₂,^{19,20} and (Cp*IrCl₂)₂,^{19,20} were prepared according to the methods in the literatures. Mononuclear complexes **12**,²¹ **13**,²² and **14**²² were synthesized according to previous literatures.

Synthesis of Triphenylenehexathiol (THT). Li (cut from a Li ribbon, 0.45 g, 65 mmol) was added to liquid NH₃ (ca. 70 mL) at –78 °C. Then hexamethylthiotriphenylene (0.86 g, 1.7 mmol) was added to the suspension, and stirred for 3.5 h at –78 °C. Degassed methanol (12 mL) was added cautiously until the blue color disappeared. The flask was allowed to warm to room temperature over 1.5 h. Degassed 10% aqueous HCl (ca. 140 mL) was added, so that white solid was precipitated. The solid was filtrated using a glass filter and washed with Et₂O and dichloromethane. Drying under vacuum gave THT as white solid (653 mg, 91%). THT decomposes rapidly under an aerobic atmosphere. Therefore, it should be handled under an inert atmosphere. Anal. Calcd for C₁₈H₁₂S₆·0.5H₂O: C, 50.31; H, 3.05. Found: C, 50.49; H, 3.05%. MALDI-TOF-MS *m/z* 421 [M+H]⁺. No ¹H NMR signal was found because of low solubility.

Synthesis of [(C₆(C₄H₂S₂CoCp*)₃)] (9**).** To a suspension of THT (42 mg, 0.10 mmol) in dichloromethane (50 mL) was added triethylamine (0.10 mL, 0.70 mmol). Then Cp*Co(CO)I₂ (0.14 g, 0.30 mmol) was added to the reaction mixture. The resultant suspension was stirred for 2 h at room temperature. Then, the suspension was filtered off, and the filtrate was evaporated. The crude product was purified by silica gel column chromatography eluted using dichloromethane/hexane (4:1 v/v), and the blue band was collected. Evaporation of the solvent gave **9** as blue powder (28 mg, 28%). ¹H NMR (500 MHz, CDCl₃) δ 2.00 (s, 45H), 8.98 (s, 6H); (500 MHz, CD₂Cl₂) δ 1.97 (s, 45H), 8.90 (s, 6H); ¹³C{¹H} NMR (126 MHz, CD₂Cl₂) δ 10.31 (s), 91.42 (s), 123.11 (s), 124.48 (s), 153.71 (s); Anal. Calcd for C₄₈H₅₁Co₃S₆·0.3C₆H₁₄·0.7CH₂Cl₂: C, 56.04; H, 5.27. Found: C, 56.26; H, 5.05%; MALDI-TOF-MS *m/z* 996 [M]⁺; HR-ESI-TOF-MS *m/z*: Calcd for C₄₈H₅₁Co₃S₆: 996.0311 [M]⁺, Found: 996.0302.

Synthesis of [(C₆(C₄H₂S₂RhCp*)₃)] (10**).** To a suspension of THT (21 mg, 0.052 mmol) in dichloromethane (15 mL) was added triethylamine (52 μL, 0.37 mmol). A dichloromethane solution (10 mL) of (Cp*RhCl₂)₂ (47 mg, 0.076 mmol) was added to the reaction mixture. The resultant suspension was stirred for 2 h at room temperature. Then, the solution was filtered off, and the filtrate was evaporated in vacuo. The crude product was purified by aluminum oxide (basic, deactivated with 10w% water) column chromatography eluted using dichloromethane, and the purple band was collected. Evaporation of the solvent gave **10** as purple powder (3.1 mg, 5.5%). ¹H NMR (500 MHz, CD₂Cl₂) δ 2.07 (s, 45H), 8.97 (s, 6H); Anal. Calcd for C₄₈H₅₁Rh₃S₆·0.2CH₂Cl₂·C₆H₁₄: C, 48.50; H, 4.54. Found: C, 48.28; H 4.76%; MALDI-TOF-MS *m/z* 1128 [M]⁺; HR-ESI-TOF-MS: *m/z*: Calcd for C₄₈H₅₁Ir₃S₆: 1127.9480 [M]⁺, Found: 1127.9502.

Synthesis of [(C₆(C₄H₂S₂IrCp*)₃)] (11**).** To a suspension of THT (210 mg, 0.50 mmol) in dichloromethane (500 mL) was added triethylamine (0.51 mL, 3.6 mmol). A dichloromethane solution (20 mL) of (Cp*IrCl₂)₂ (598 mg, 0.75 mmol) was added to the reaction mixture. The resultant suspension was stirred for 3 h at room temperature. Then the solution was filtered off, and the filtrate was evaporated in vacuo. The crude product was purified by silica gel column chromatography eluted using dichloromethane/hexane (4:1 v/v), and the second yellow-orange band was collected. Evaporation of the solvent gave **11** as gold powder (423 mg, 61%). ¹H NMR (500 MHz, CDCl₃) δ 2.19 (s, 45H), 9.27 (s, 6H); (500 MHz, CD₂Cl₂) δ 2.18 (s, 45H), 9.21 (s, 6H); ¹³C{¹H} NMR (126 MHz, CD₂Cl₂) δ

10.14 (s), 91.80 (s), 122.97 (s), 125.52 (s), 152.10 (s); Anal. Calcd for C₄₈H₅₁Ir₃S₆: C, 41.27; H, 3.68. Found: C, 41.62; H, 3.96%; MALDI-TOF-MS *m/z* 1397 [M]⁺.

■ ASSOCIATED CONTENT

📄 Supporting Information

Crystallographic parameters of **11**, frontier orbitals and their energies for **12**, **9**, and **3**, TD-DFT calculation for **12**, **9**, and **3**, frontier orbitals and their energies for **9–11**, TD-DFT calculation for **10** and **11**, deconvolution of the differential pulse voltammograms of **9–11**, UV–vis–NIR spectral change of **9** upon reduction to **9⁻**, **9²⁻**, and **9³⁻**, and cif file for **11**. This material is available free of charge via the Internet at <http://pubs.acs.org>.

■ AUTHOR INFORMATION

✉ Corresponding Author

*E-mail: sakamoto@chem.s.u-tokyo.ac.jp (R.S.), nishihara@chem.s.u-tokyo.ac.jp (H.N.).

Notes

The authors declare no competing financial interest.

■ ACKNOWLEDGMENTS

This work was supported by Grants-in-Aid from MEXT of Japan [Nos. 24750054 and 21108002, area 2107 (Coordination Programming)], JSPS Research Fellowship for Young Scientists, and the Global COE Program for Chemistry Innovation.

■ REFERENCES

- (1) (a) Murahashi, T.; Jujimoto, M.; Oka, M.; Hashimoto, Y.; Uemura, T.; Tatsumi, Y.; Nakao, Y.; Ikeda, A.; Sakaki, S.; Kurosawa, H. *Science* **2006**, *313*, 1104. (b) Inagaki, A.; Takemori, T.; Tanaka, M.; Suzuki, H. *Angew. Chem., Int. Ed.* **2000**, *39*, 404–406. (c) Bruce, M. I.; Zaitseva, N. N.; Skelton, B. W.; White, A. H.; Fox, M. A.; Low, P. J. *Dalton Trans.* **2010**, 1222–1234. (d) Taylor, N. J.; Chieh, P. C.; Carty, A. J. *J. Chem. Soc., Chem. Commun.* **1975**, 448. (e) Eisenberg, R. *Coord. Chem. Rev.* **2011**, *255*, 825–836.
- (2) (a) Yoon, J.; Mirica, L. M.; Stack, T. D. P.; Solomon, E. I. *J. Am. Chem. Soc.* **2004**, *126*, 12586–12595. (b) Baffer, C.; Orto, M.; Pantazis, D. A.; Duboc, C.; Blackman, A. G.; Blondin, G.; Neese, F.; Deronzier, A.; Collomb, M.-N. *Inorg. Chem.* **2009**, *48*, 10281. (c) Müller, A.; Jostes, R.; Eltzner, W.; Nie, C.-S.; Diemann, E.; Bögge, H.; Zimmermann, M.; Dartmann, M.; Reinsch-Vogell, U.; Che, S.; Cyvin, S. J.; Cyvin, B. N. *Inorg. Chem.* **1985**, *24*, 2872–2884. (d) Rivera-Carrillo, M.; Chakraborty, I.; Mezei, G.; Webster, R. D.; Raptis, R. G. *Inorg. Chem.* **2008**, *47*, 7644–7650. (e) Astruc, D. *Acc. Chem. Res.* **1997**, *30*, 383–391.
- (3) (a) Ferrer, S.; Lloret, F.; Bertomeu, I.; Alzuet, G.; Borrás, J.; García-Granda, S.; Liu-González, M.; Haasnoot, J. G. *Inorg. Chem.* **2002**, *41*, 5821–5831. (b) Sant, S.; Orian, L.; Bisello, A.; Scapinello, M.; Benetollo, F.; Ganis, P.; Ceccon, A. *Angew. Chem., Int. Ed.* **2008**, *47*, 5331–5334. (c) Weyland, T.; Lapinte, C.; Frapper, G.; Calhorda, M. J.; Halet, J. F.; Toupet, L. *Organometallics* **1997**, *16*, 2024–2031. (d) Burini, A.; Mohamed, A. A.; Fackler, J. P. *Comments Inorg. Chem.* **2003**, *24*, 253–280. (e) Bergen, L. A.; Faia, M. C.; Crawford, N. R. M.; Long, J. R. *Inorg. Chem.* **2006**, *45*, 6378–6386.
- (4) (a) Nishihara, H.; Okuno, M.; Kogawa, N.; Aramaki, K. *J. Chem. Soc., Dalton Trans.* **1998**, 2651–2656. (b) Shibata, Y.; Zhu, B.-H.; Kume, S.; Nishihara, H. *Dalton Trans.* **2009**, 1939–1943. (c) Kambe, T.; Tsukada, S.; Sakamoto, R.; Nishihara, H. *Inorg. Chem.* **2011**, *50*, 6856–6858. (d) Tsukada, S.; Shibata, Y.; Sakamoto, R.; Kambe, T.; Ozeki, T.; Nishihara, H. *Inorg. Chem.* **2012**, *51*, 1228. (e) Sakamoto, R.; Tsukada, S.; Nishihara, H. *Dalton Trans.* **2012**, *41*, 10123.
- (5) (a) Okuno, M.; Aramaki, K.; Nakajima, S.; Watanabe, T.; Nishihara, H. *Chem. Lett.* **1995**, *24*, 585. (b) Okuno, M.; Aramaki, K.; Nishihara, H. *J. Electroanal. Chem.* **1997**, *438*, 79. (c) Nihei, M.;

- Nankawa, T.; Kurihara, M.; Nishihara, H. *Angew. Chem., Int. Ed.* **1999**, *38*, 1098. (d) Nakagawa, N.; Yamada, T.; Murata, M.; Sugimoto, M.; Nishihara, H. *Inorg. Chem.* **2006**, *45*, 14. (e) Murata, M.; Habe, S.; Araki, S.; Namiki, K.; Yamada, T.; Nakagawa, N.; Nankawa, T.; Nihei, M.; Mizutani, J.; Kurihara, M.; Nishihara, H. *Inorg. Chem.* **2006**, *45*, 1108. (f) Nakagawa, N.; Murata, M.; Sugimoto, M.; Nishihara, H. *Eur. J. Inorg. Chem.* **2006**, 2129. (g) Muratsugu, S.; Sodeyama, K.; Kitamura, F.; Sugimoto, M.; Tsuneyuki, S.; Miyashita, S.; Kato, T.; Nishihara, H. *J. Am. Chem. Soc.* **2009**, *131*, 1388. (h) Muratsugu, S.; Sodeyama, K.; Kitamura, F.; Tsukada, S.; Tada, M.; Tsuneyuki, S.; Nishihara, H. *Chem. Sci.* **2011**, *2*, 1960. (i) Tsukada, S.; Sakamoto, R.; Nishihara, H. *Chem. Lett.* **2012**, *41*, 357–359. (j) Zhu, B.-H.; Shibata, Y.; Muratsugu, S.; Yamanoi, Y.; Nishihara, H. *Angew. Chem., Int. Ed.* **2009**, *48*, 3858.
- (6) (a) Randic, M. *Chem. Rev.* **2003**, *103*, 3449–3605. (b) Milan, R. *Int. J. Quantum Chem.* **1998**, *63*, 585–600. (c) Poater, J.; Fradera, X.; Duran, M.; Solà, M. *Chem.—Eur. J.* **2003**, *9*, 400–406. (d) Pauling, L. *J. Chem. Phys.* **1936**, *4*, 673–677.
- (7) (a) Adam, D.; Schuhmacher, P.; Simmerer, J.; Häussling, L.; Siemensmeyer, K.; Eitzbach, K. H.; Ringsdorf, H.; Haarer, D. *Nature* **1994**, *371*, 141–143. (b) Van de Craats, A. M.; Warman, J. M.; De Haas, M. P.; Adam, D.; Simmerer, J.; Haarer, D.; Schuhmacher, P. *Adv. Mater.* **1996**, *8*, 823–826. (c) van de Craats, A. M.; De Haas, M. P.; Warman, J. M. *Synth. Met.* **1997**, *86*, 2125–2126.
- (8) (a) Li, K.; Xu, Z.; Fettingner, J. C. *Inorg. Chem.* **2004**, *43*, 8018–8022. (b) Li, K.; Xu, Z.; Xu, H.; Ryan, J. M. *Chem. Mater.* **2005**, *17*, 4426–4437. (c) Xu, Z.; Li, K.; Fettingner, J. C.; Li, J.; King, M. M. *Cryst. Growth Des.* **2005**, *5*, 423–425. (d) Li, K.; Xu, Z.; Xu, H.; Carroll, P. J.; Fettingner, J. C. *Inorg. Chem.* **2006**, *45*, 1032–1037. (e) Li, K.; Huang, G.; Xu, Z.; Carroll, P. J. *J. Solid State Chem.* **2006**, *179*, 3688–3694.
- (9) Tan-Sien-Hee, L.; Mesmaeker, A. K.-D. *J. Chem. Soc., Dalton Trans.* **1994**, 3651–3658.
- (10) Grange, C. S.; Meijer, A. J. H. M.; Ward, M. D. *Dalton Trans.* **2010**, *39*, 200–211.
- (11) ORTEP drawing was created using ORTEP-3 for Windows: Farrugia, L. J. *J. Appl. Crystallogr.* **1997**, *30*, 565.
- (12) (a) Creutz, C. *Prog. Inorg. Chem.* **1983**, *30*, 1. (b) Fellows, E. A.; Keene, F. R. *J. Phys. Chem. B* **2007**, *111*, 6667–6675. (c) Chung, M.-C.; Gu, X.; Etzenhouser, B. A.; Spuches, A. M.; Rye, P. T.; Seetharaman, S. K.; Rose, D. J.; Zubietta, J.; Sponsler, M. B. *Organometallics* **2003**, *22*, 3485–3494. (d) Linseis, M.; Zális, S.; Zabel, M.; Winter, R. F. *J. Am. Chem. Soc.* **2012**, *134*, 16671–16692. (e) Man, W. Y.; Vincent, K. B.; Spencer, H. J.; Yufit, D. S.; Howard, J. A. K.; Low, P. J. *J. Cluster Sci.* **2012**, *23*, 855–872. (f) Mücke, P.; Winter, R. F.; Novak, I.; Kowalski, K. J. *Organomet. Chem.* **2012**, *717*, 14–22.
- (13) Hush, N. S. *Coord. Chem. Rev.* **1985**, *64*, 135–157.
- (14) Sheldrick, G. M. *SHELXS-97, Program for Crystal Structure Solution*; University of Göttingen: Göttingen, Germany, 1997.
- (15) Frisch, M. J.; Trucks, G. W.; Schlegel, H. B.; Scuseria, G. E.; Robb, M. A.; Cheeseman, J. R.; Scalmani, G.; Barone, V.; Mennucci, B.; Petersson, G. A.; Nakatsuji, H.; Caricato, M.; Li, X.; Hratchian, H. P.; Izmaylov, A. F.; Bloino, J.; Zheng, G.; Sonnenberg, J. L.; Hada, M.; Ehara, M.; Toyota, K.; Fukuda, R.; Hasegawa, J.; Ishida, M.; Nakajima, T.; Honda, Y.; Kitao, O.; Nakai, H.; Vreven, T.; Montgomery, Jr., J. A.; Peralta, J. E.; Ogliaro, F.; Bearpark, M.; Heyd, J. J.; Brothers, E.; Kudin, K. N.; Staroverov, V. N.; Keith, T.; Kobayashi, R.; Normand, J.; Raghavachari, K.; Rendell, A.; Burant, J. C.; Iyengar, S. S.; Tomasi, J.; Cossi, M.; Rega, N.; Millam, J. M.; Klene, M.; Knox, J. E.; Cross, J. B.; Bakken, V.; Adamo, C.; Jaramillo, J.; Gomperts, R.; Stratmann, R. E.; Yazyev, O.; Austin, A. J.; Cammi, R.; Pomelli, C.; Ochterski, J. W.; Martin, R. L.; Morokuma, K.; Zakrzewski, V. G.; Voth, G. A.; Salvador, P.; Dannenberg, J. J.; Dapprich, S.; Daniels, A. D.; Farkas, O.; Foresman, J. B.; Ortiz, J. V.; Cioslowski, J.; Fox, D. J. *Gaussian 09, Revision B.01*; Gaussian Inc.: Wallingford, CT, 2010.
- (16) Cossi, M.; Scalmani, G.; Rega, N.; Barone, V. *J. Chem. Phys.* **2002**, *117*, 43–54.
- (17) Xu, Z.; Li, K.; Fettingner, J. C.; Li, J.; King, M. M. *Cryst. Growth Des.* **2005**, *5*, 423–425.
- (18) Frith, S. A.; Spencer, J. L. *Inorg. Synth.* **1985**, *23*, 15–16.
- (19) Shibata, Y. Thesis for the Degree of Doctor of Science, The University of Tokyo, Tokyo, Japan, 2008.
- (20) Kang, J. W.; Moseley, K.; Maitlis, P. M. *J. Am. Chem. Soc.* **1969**, *91*, 5970–5977.
- (21) Heck, R. F. *Inorg. Chem.* **1968**, *7*, 1513–1516.
- (22) Xi, R.; Abe, M.; Suzuki, T.; Nishioka, T.; Isobe, K. *J. Organomet. Chem.* **1997**, *549*, 117–125.